Molecular BioSystems

Accepted Manuscript

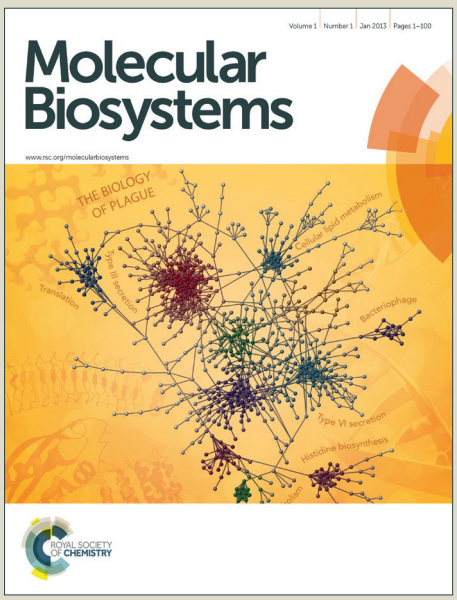

ROYAL SOCIETY OF CHEMISTRY

www.rsc.org/molecularbiosystems

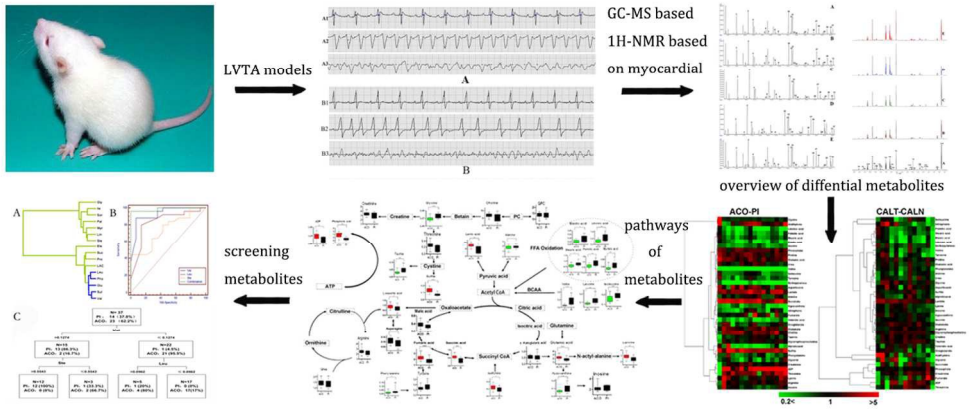

135x59mm (300 x 300 DPI)

Non-targeted metabolomics identified a common metabolic signature of lethal ventricular tachyarrhythmia (LVTA) in two rat models

Xingxing Wang[1]. Dian Wang[1]. Xiaojun Yu[1]. Guohong Zhang[2]. Jiayan Wu[1]. Guanghui Zhu[1]. Ruibing Su[1]. Junyao Lv[1]

Running title: Metabolic feature of lethal ventricular tachyarrhythmia

[1]Department of Forensic Medicine, Shantou University Medical College

[2] Department of Pathology, Shantou University Medical College

Xingxing Wang and Dian Wang have contributed equally.

Correspondence to Dian Wang: Department of Forensic Medicine, Shantou University Medical College，22 Xinling Road, Shantou, 515041, China.

Phone and Fax: (+86)754-8890-0433.

E-mail: g_dwang@stu.edu.cn

Acknowledgements This work was supported by the Natural Science Foundation (2015A408119346049) and Science and Technology Innovation project (2013KJCX0076) of Guangdong Province, and Characteristic Key Project of Pathology and Pathophysiology, Ministry of Finance, China.

Abstract

Lethal ventricular tachyarrhythmia (LVTA) is the predominant underlying mechanism of sudden cardiac death (SCD). The aim of this study is to characterize the metabolic features of myocardia following LVTA, and identify potential biomarkers to diagnose LVTA. We developed two LVTA rat models induced by aconitine injection or coronary artery ligation, which represent cardiac ion channel disease-related and cardiac ischemia-related SCD, respectively. The myocardial metabolic profile was investigated by gas chromatography-mass spectrometry and proton nuclear magnetic resonance-based metabolomics. Twenty-three aconitine-injected and 14 coronary artery ligation-treated rats developed LVTA SCD. A total of 38 differential metabolites of myocardia were identified in aconitine-induced LVTA rats, of which 31 metabolites showed a similar change in coronary artery ligation-related LVTA rats. Fatty acids (stearic, palmitic, linoleic, elaidic, myristic) and branched-chain amino acids (valine, leucine, and isoleucine) were the most down-regulated metabolites. Furthermore, elevated ADP, phosphate, lactate, glutamate, aspartate, threonine, choline and arginine were also observed. Major pathways regarding these dysregulated metabolites post LVTA are energy excessive consumption and deficit, ionic imbalance, oxidative stress, cardiac cytotoxicity and membrane injury. Valine, stearic acid and leucine collectively enable a precision of 92.9% to distinguish LVTA from its control, and are correlated with several arrhythmia indices. Our results uncovered a common metabolic feature of LVTA in myocardia in two rat models, which represent cardiac ion channel disease and cardiac ischemia, respectively. L-valine, L-leucine and stearic acid jointly confer good potential for distinguishing LVTA, which might be potential biomarkers of LVTA-related SCD.

Keywords Lethal ventricular tachyarrhythmia, sudden cardiac death, non-targeted metabolomics, fatty acid, branched-chain amino acid

Introduction

Sudden cardiac death (SCD) remains a major public health problem, affecting more than 3 million people worldwide,[1] with a reported overall incidence of 0.418 ‰ per year in China,[2] and is responsible for around 300,000 and 60,000 deaths annually in the USA and the UK, respectively.[3, 4] The predominant underlying mechanism and responsibility for death is lethal ventricular tachyarrhythmia (LVTA), including ventricular tachycardia (VT) and ventricular fibrillation (VF), no matter what the pathological basis is.[5] However, the principal mechanisms for LVTA occurrence are not yet fully understood. Systematic understanding of LVTA metabolism could help identify the underlying mechanisms of LVTA, and provide diagnostic markers and potential therapeutic targets for LVTA and its relative death. Metabolomics is a top-down platform in the field of systems biology, which focuses on dynamic changes of small molecules in response to the disturbance of the organism.[6] Non-targeted metabolomics approaches are being widely used for the discovery of new biomarkers and mechanisms. These approaches have also been extensively utilized to investigate the metabolic profiling and biomarkers of cardiovascular diseases.[7]

Myocardium is unavailable in clinical setting, thus, LVTA animal models is an essential avenue to explore its metabolic mechanism. Previous animal VT and/or VF models include electricity-elicited and hypoxia-induced VF in perfused isolated rat heart,[8, 9] and myocardial ischemia-induced VF in swine,[10] showing metabolic alterations in VT or VF, such as decreases in ATP, phosphate creatine and glycogen, increases in glucose-6-phosphate, lactate,[8] and intracellular Na^+ accumulation.[9] However, these models cannot reflect an overall metabolic change after VF, or are costly. In this study, we developed two LVTA rat models, one induced by aconitine injection and the other elicited by coronary artery ligation (CAL)-induced myocardial ischemia. Both have a relatively higher incidence of LVTA in our pre-experiments, and represent two major LVTA-triggering pathological bases, including cardiac ion channel disease and myocardial ischemia. Then, the global metabolic characteristics of myocardia in the two models were

explored and compared using gas chromatography-mass spectrometry (GC-MS) and proton nuclear magnetic resonance (1H-NMR)-based metabolomics. On basis of differentially expressed metabolites, the metabolic pathways and interactive networks and their potential to diagnose LVTA were analyzed. In addition, an association analysis was performed between the relative amounts of differential metabolites and arrhythmia indices, including VT, VF duration, and arrhythmia score, to partially validate related LVTA biomarkers.

Materials and Methods

Animals

This study was approved by the Medical Animal Care & Welfare Committee at Shantou University Medical College. All procedures were carried out in accordance with the Helsinki Declaration.

Adult male Sprague–Dawley rats (weighing 250-500g) were supplied by the Animal Research Center of Shantou University Medical College, and were kept in plastic cages at room temperature with a 12-h light/dark cycle and a relative humidity of 50-60%. The rats had access to rodent chow and tap water ad libitum. Rats were randomly divided into two groups for the establishment of two LVTA models and their controls, with different numbers in each group.

Establishment of LVTA models

Aconitine was used and CAL was performed to establish two rat LVTA models, which were defined as Model I and Model II, respectively. Model I (LVTA-SCD group): rats were anesthetized by peritoneal injection of 3% pentobarbital sodium (30 mg/kg) and the lead II electrocardiogram (ECG) was monitored using a BL-420 Biological Functional Experimental System (Chengdu Taimeng Co. Ltd., China). Subsequently, rats were injected with aconitine (50 μg/mL in saline, 100 μL for each rat) through their tail veins. Typically, premature ventricular beat and subsequent VT, VF and death (LVTA) occurred in 1-5 minutes after the injection. Rats that were over-anesthetized

with pentobarbital sodium to death served as the control for the ACO-LVTA group. Immediately after death, rats were dissected and whole hearts were harvested and stored at -80℃.

Model II (CAL-T): rats were anesthetized and monitored by ECG, as in Model I, then left anterior descending CAL was performed as previously described.[11] Briefly, after the onset of artificial ventilation by endotracheal intubation through a small animal ventilator (Shanghai ALCOTT BIOTECH CO., LTD, China), and subsequent left thoracotomy, the pericardium was opened and the heart was exteriorized. The left coronary artery was ligated from the root as soon as possible, in the case of perfect ligation, and then the heart was immediately placed back into the thoracic cavity. The T wave of ECG should rise dramatically after CAL, verifying the success of ligation and the occurrence of myocardial ischemia. Rats that developed VT and subsequent VF, and that died soon thereafter, were designated as the typical LVTA group (CAL-T). Rats that did not develop LVTA, but bradycardia, and died of severe atrioventricular block, were served as the control group (CAL-N). Other rats that just had paroxysmal VT and/or VF, and then returned to a normal sinus heart rate for 70 minutes (the endpoint of investigation in this study) after CAL were defined as the intermediate group (CAL-M), and were sacrificed by clamping the aorta. Hearts were retrieved and treated the same as in Model I. Right ventricular myocardia was consistently used for the two detection methods below to exclude the effect of direct myocardial ischemia caused by CAL on the comparison of various groups and the variation due to different parts of the myocardium. The recorded ECGs were further used to analyze the severity of arrhythmia, and were quantified and scored following the guidelines known as The Lambeth Convention guidelines.[12]

Metabolic profiling by GC-MS

The GC-MS-based metabolic profile of myocardia from all experimental rats was analyzed according to previous references.[13, 14] Briefly, 30 mg of myocardium was extracted with methanol, oximated with methoxyamine (15

mg/ml in pyridine), and derivatized by MtBSFA (1% TMCS). Then a 1 μL aliquot of the derivatized solution was analyzed by a GC-MS system consisting of an Agilent 7890A GC system, connected to an Agilent 5975C single quadrupole MSD. Before detection, precision and stability were evaluated to ensure the quality of analysis. Acquired chromatograms were analyzed by ChemStation software. Metabolites were identified directly by comparison to the similarities and differences between the theoretical mass spectra and experimental mass spectra acquired in the 2.0 NIST library. Details can be found in the Supplementary Experimental Procedures.

Metabolic profiling by 1H-NMR

1H-NMR-based metabolic profile of myocardia, from 16 ACO-LVTA rats, 13 CAL-T rats, 14 CAL-M rats and their control rats, which were randomly selected from two models, respectively, was analyzed according to previous reports.[14, 15] Briefly, 30 mg of myocardium was homogenized and extracted by perchloric acid, made into a dry powder with a Moduloyd freeze dryer, and dissolved in D2O, then analyzed by an NMR spectrometer (600.13 MHz, Bruker Biospin) using a NOESYPRID spectrum. The 1H-NMR 1D spectra were analyzed using MestReNova software. Metabolites in the spectra were identified by matching with information in relevant literature and comparison to public databases, such as the BioMagResBank Database and the Human Metabolome Database.[14, 15] The relative contents of metabolites were calculated with the following formula according to reference: Cm=TIm/TItsp×Np/9×Ctsp, where TIm and TItsp stand for the total integrals of metabolite and TSP, respectively. Np and 9 represent the number of protons of the metabolite and TSP, respectively. Cm and Ctsp stand for the concentrations of metabolites and TSP, respectively.[16] Details can be found in the Supplementary Experimental Procedures.

Data processing and analysis

The data matrix from 1H-NMR and GC-MS was imported into a SIMCA-P program (version13.0, Umetrics) for

multivariate analysis. Principal component analysis (PCA) and partial least squares discriminate analysis (PLS-DA) were applied with unit variance (UV) scaling. The parameters of the models, such as the R2X, R2Y, and Q2Y, and the R2Y-, Q2Y-intercepts, were analyzed to ensure the quality of the multivariate models and to avoid the risk of over-fitting. [17]

The Cluster 3.0 and Treeview1.1.6 software packages were used to make a heat map to represent the relative amount of each metabolite, and to analyze their hierarchical cluster. An interactive network was constructed using Cytoscape software package, version 3.1.1.

A receiver operating characteristic curve (ROC) analysis was performed for selecting the optimal cut-off point score for each metabolite, and then the values of metabolites were categorized to find an interaction between metabolites by the multifactor dimensionality reduction (MDR).[18] After identification of the most different core metabolites, classification and regression tree (CRT) analysis was performed to explore the most valuable metabolites for distinguishing LVTA from the control.[19]

Univariate statistics were performed, using SPSS17.0 software, to compare the relative amounts of metabolites, between LVTA groups and their controls, by ANOVA and t-test after validation by the Kolmogorov-Smirnov test. The normalized amount of each metabolite was plotted in a histogram using an Origin software package (version 5.0). The associations between relative amount of metabolites and arrhythmia score or VT VF duration(s) were analyzed by the bivariate correlation of Spearman.

Results

LVTA models and ECG features

LVTA occurred in 23 out of 24 rats injected with aconitine, with the duration of VT, VF and VT+VF being 25 s (5-41 s), 103 s (50-174 s) and 133 s (86-213 s), respectively, and with an arrhythmia score between 5 and 6. By

comparison, severe bradycardia and atrioventricular block, instead of LVTA, occurred in fourteen control rats, where death due to over-anesthetization by pentobarbital sodium occurred. All values for the above ECG characteristics of the control were zero (all $P<0.001$ when comparing with related indices of LVTA rats, Fig1s. A, D and Supplementary Table1). The results confirmed successful establishment of LVTA induced by aconitine.

LVTA occurred in 14 out of 36 rats (38.9%) that had undergone CAL (CAL-T). The durations of VT, VF, VT+VF, were 47 s (0-210 s), 162 s (11-440 s), 228.5 s (75-446 s), and the arrhythmia score ranged from 5 to 7. Fifteen CAL-treated rats only had paroxysmal VT and/or VF, followed by a normal sinus rhythm up to 70 minutes after CAL (CAL-M), when the experiment was terminated. The durations of VT, VF and VT+VF were 34 s (0-206 s), 27 s (0-115 s), 71 s (3-278 s), respectively, and the arrhythmia score ranged from 3 to 6. All were significantly lower than those of the CAL-T group ($P<0.001$), except for VT duration ($P>0.05$). Seven CAL-treated rats did not proceed to ventricular arrhythmia, but rather to bradycardia, and then died of severe atrio-ventricular block (CAL-N), with the durations of VT, VF and VT+VF being zero and the arrhythmia score between 0-2 (Fig1s. B, C and Supplementary Table 1). These results verify the establishment of CAL-induced LVTA, and also illustrate the rationality of the grouping of the CAL-treated rats.

Metabolic profile of the myocardia suffering from LVTA

In this study, two non-targeted metabolomics strategies, based on GC-MS and 1H-NMR, were applied for metabolic profiling of LVTA-myocardia. Validations of the GC-MS detection, including precision and stability, showed relative metabolomics was reliable. The typical base peak chromatograms and 1H- NMR spectra illustrated the difference in metabolic profiles between ACO-LVTA and its control, and among three CAL groups, respectively (Supplementary Figs. S1 and S2). A total of 38 metabolites and 29 metabolites had been identified and quantified from GC-MS spectra and 1H-NMR spectra, respectively.

To analyze the differences in metabolic profile, GC-MS and 1H-NMR data from the two LVTA models and their controls were imported into the SIMCA-P 13.0 software Package. Subsequently, partial least squares-discrimination analyses (PLS-DAs) were applied to the classification of LVTA and its controls. The PLS-DA score plot illustrated ACO-LVTA myocardia were clearly separated from the control in both GC-MS and 1H-NMR modes (Figs. 2A, B). The cumulative R^2Y and Q^2 were 0.917 and 0.746, and 0.804 and 0.285 in GC-MS and 1H-NMR modes, respectively, when two components were calculated. No over-fitting was observed according to the results of the 200 times of chance permutation. The R^2Y-intercepts were 0.536 and 0.695, and the Q^2-intercepts were -0.455 and -0.125 in GC-MS and 1H-NMR modes, respectively (Supplementary Figs. S3A, B). There were also distinct differences between the CAL-T, CAL-M and CAL-N metabolites in both modes (Figs. 2C, D). The cumulative R^2Y and Q^2 were 0.850 and 0.654, and 0.378 and 0.149 in GC-MS and 1H-NMR modes, respectively, when the three components were calculated. The R^2Y-intercepts were 0.238 and 0.263, and the Q^2-intercepts were -0.211 and -0.100 in GC-MS and 1H-NMR modes, respectively (Supplementary Figs. S4C, D). The results further confirm a significant difference in metabolic profiles of myocardia with ACO-LVTA compared to those of control, and a remarkable difference in metabolic profile of myocardia when comparing CAL-LVTA from those of CAL-N and CAL-M groups in both modes.

Differential metabolites in the two LVTA models and their comparisons

Two strategies were used to define the potential differential metabolites for distinguishing the LVTA and its control, including multivariate and univariate modes. For the multivariate mode, a PLS-DA S-plot was applied to find the ions in the GC-MS data, or the spectral integrals in the 1H-NMR data, with a variable importance in the projection (VIP) of more than 0.75. In the univariate method, the relative amounts of metabolites in the different groups were compared by t-test, and those with a $P<0.05$ were selected.

After integrating data of GC-MS and 1H NMR, 38 differential metabolites were found (P<0.05, and/or VIP>0.75) in aconitine-induced LVTA, compared with its peer control. Among these, 31 had the same change trend seen in CAL-induced LVTA. To analyze these 38 differential metabolites globally, the Cluster 3.0 and Treeview1.1.6 software packages were used to make a heat map according to a ratio of the content of each differential metabolite in each LVTA rat to average content of this metabolite in their non-LVTA controls (Fig. 3). The metabolites were clustered according to their Pearson correlation coefficients. Overall, in both models, the changes of these metabolites in LVTA myocardia were quite different from those samples without LVTA.

In Model I, sixteen metabolites were identified with a VIP>0.75, according to the GC-MS data when ACO-LVTA was compared with its control, whereas data from 1H-NMR identified fifteen metabolites. Both included lactate and L-valine. Nineteen metabolites from the GC-MS analysis were significantly different (p<0.05) between ACO-LVTA and its control, whereas, eight metabolites were shown to be different by 1H-NMR. Both methods of detection identified lactate, L-valine, isoleucine and L-leucine (Table 1).

In Model II, five metabolites were found with a VIP>0.75, according to the GC-MS data when the CAL-T group was compared with the CAL-N group, whereas 1H-NMR showed ten. Only two metabolites from the GC-MS-based data were found to be significantly different (P<0.05) between CAL-T and CAL-N, which are lactate and stearic acid. Five metabolites displayed significant changes, as detected by 1H-NMR.

More remarkably, different metabolites were found in Model I than in Model II (38:15), probably due to the effects of CAL itself to myocardia metabolism. However, 31 of these differential metabolites (81.5%) had the same trend of change in both models, implying a common metabolic consequence between these two LVTA models.

Metabolic pathways of LVTA in the myocardium

To explore LVTA-related metabolic mechanisms in the myocardium, a map of LVTA-related metabolic pathways

was built according to the relative amount of differential metabolites between ACO-LVTA and its control (Fig. 3), based on the knowledge of these differential metabolites and an online database of metabolic pathways (Kyoto Encyclopedia of Genes and Genomes). Several metabolic pathways were modified by induction of LVTA. For example, a remarkable decrease of all detected fatty acids, including palmitic, linoleic, elaidic, stearic, and myristic acids, reflects a huge expenditure of fatty acids and an enhancement of β-oxidation. A significant decline of three branched-chain amino acids (BCAA), specifically L-valine, L-leucine, and isoleucine, was also observed, representing consumption due to high catabolism. Tricarboxylic acid cycle (TCA) metabolites, such as fumarate, succinate and malate increased in LVTA-myocardia, indicative of TCA activity and aerobic oxidation. Lactate increased in LVTA of both models, as detected by either GC-MS or 1H-NMR, implying an enhancement of anaerobic oxidation and its close relationship with LVTA. In addition, ATP degradation products, ADP and phosphate, increased remarkably, implying higher energy expenditure during LVTA.

To further investigate the latent relationship of the differential metabolites, a correlation network diagram was constructed using the Cytoscape software after interactive correlation coefficients of these metabolites were calculated by the R 3.2.0 software package (Supplementary Fig. S5). Results showed that all detected free fatty acids and BCAAs were located in the center of the correlation network, suggestive of a strong correlation and the leading role of these metabolites in distinguishing LVTA from control.

Diagnostic potential of differential metabolites found in myocardia

Biomarkers could help explore the determining factor for the occurrence of LVTA and uncover related therapeutic targets for clinical application. In this study, biomarkers were preliminarily screened by a metabolomics strategy, identifying candidate biomarkers as those metabolites that simultaneously fulfilled the criteria of having a VIP>1.0 and $P<0.05$. Metabolites satisfying these criteria were lactate, L-valine, isoleucine, L-leucine, palmitic acid, linoleic

acid, and stearic acid in Model I, and lactate in model II. Second, sixteen differential metabolites that had a ROC curve AUC value of more than 0.74 were selected. Then MDR was performed. MDR was designed specifically to identify interactions among discrete variables that influence a binary outcome.[18] As illustrated in Fig. 5A, sulfite and L-valine, glutamate, L-leucine and phosphate were clustered, namely, they have the same core value to discriminate LVTA from its control. Similarly, succinate and proline were clustered, and combined with lactate to make up a big cluster with the above one. Sulfite and L-valine were equally central for distinguishing LVTA. Therefore, L-valine, L-leucine, lactate, succinate and stearic acid, which represented relative branch, were chosen to perform a CRT. As a result, succinate and lactate were filtered out, and L-valine, stearic acid and L-leucine were chosen to make a classification tree enabling the highest precision of 92.9% and AUC value of 0.986 (Fig. 5 B), as compared with use of single metabolites to distinguish LVTA from its control. The classifier chooses the subject score based on L-valine to make the first split (Fig. 5C). In the left and right subtree, the classifier goes on to test the rest of the subjects based on stearic acid and L-leucine, respectively.

Association analyses

We performed association analyses between the relative amount of the important differential metabolites and arrhythmia indices, which included the duration of VT, VF, VT+VF, and arrhythmia score, to in part validate the candidate LVTA biomarkers. Table 3 shows 14 out of the 16 top AUC metabolites were significantly correlated with all or partial arrhythmia indices. Among these, L-valine, stearic acid, and L-leucine, were negatively associated with all arrhythmia indices with most correlation coefficients being greater than 0.4.

Discussion

A systematic understanding of LVTA metabolism may facilitate the exploration of LVTA mechanism. However, such understanding remains a challenge.[20] This study investigates the LVTA metabolome in two rat models, using

GC-MS- and 1H-NMR-based non-targeted metabolomics.

LVTA rat models

We successfully developed two LVTA rat models. Model I is produced by aconitine injection to represent cardiac ion channel disease-related SCD. Aconitine mainly act on sodium or potassium channels of myocardia and can make a few ventricular myocytes be separate pacemakers, then resulting in heterogeneity of conduction and refractory period among various ventricular myocytes, by which can induce LVTA and SCD. Little amount of aconitine was used in this study, suggesting that the effect of aconitine itself on myocardial metabolism was slight and negligible. Thus, the model I can really represent cardiac ion channel disease-related SCD. Model II is elicited by CAL-related myocardial ischemia to represent coronary heart disease-related SCD, which is the most common form of structural heart disease-related SCD. In this model, rats that performed with CAL without VT and VF were served as control, which can exclude the effect of pre-treated factors such as anaesthesia and CAL injury per se, making LVTA an independent influential factor on myocardial metabolism. Importantly, we simultaneously analyzed and compared LVTA-related metabolic profiles of these two models, attempting to find some common metabolic characteristics of them. To a certain extent, such a design, could validate mutually, is more likely to discover LVTA-independent metabolic biomarkers. Previous studies suggest various arrhythmia-induced cardiac pathologies share common genetic variants, such as KASQ2 and KCNE1.[3, 21] However, it is not clear whether these two LVTA-triggering pathological bases share common metabolic alterations. The current results show that 31 out of the 38 differential metabolites in aconitine-induced LVTA demonstrate a same trend of change in ischemia-related LVTA, and support the potential effect of metabolic determinants on these models. Common differential metabolites include 13 amino acids, five long-chain fatty acids, five energy metabolic products, and eight other metabolites (Table 1). The myocardial metabolic landscape of LVTA, as compared with their controls, is illustrated by the PLS-DA score plot,

heat map and metabolic pathway (Figs. 2, 3, 4).

Metabolic features of myocardia undergoing LVTA

The initial metabolic feature of myocardial metabolism during LVTA is the down-regulation of all fatty acids detected, including stearic, palmitic, linoleic, elaidic, and myristic acids (Figs. 2, 3), indicative of huge overall consumption of fatty acids during LVTA. Fatty acids are known to be responsible for 60-80% of the oxidation fuel for the heart under normal physical conditions.[22, 23] Under conditions of lethal arrhythmia, including VT and VF, rapid myocardial contraction and fibrillation increase the consumption of fatty acids to meet the extreme need for energy, leading to declining levels of fatty acids and enhancement of β-oxidation [8] and increasing levels of ADP, similar to that occurring in myocardial ischemia.[24] Second, the resulting lower fatty acid content may alter the fluidity and structure of cardiac membrane, which affects the flux of Ca^{2+} or other ions through specific channels, inducing arrhythmia, or deteriorating an existing ventricular arrhythmia to LVTA.[25] The injury of cardiac membrane during LVTA can also be supported by simultaneous increased choline and glycerophosphocholine (Fig. 4, Table 1), which might accumulate from the breakdown of phosphatidylcholine, a major component of membrane phospholipid bilayer. Third, polyunsaturated fatty acids have been proven to be able to prevent VF caused by ischemia/reperfusion, mainly through the modulation of cardiac channel activity, such as voltage-gated Na_+ channels and L-type Ca^{2+} channels. Polyunsaturated fatty acids include linoleic, linolenic acid and their derivatives, such as arachidonic acid, docosahexaenoic acid and eicosapentaenoic acid. Thus, the lower level of linoleic acid during LVTA may lead to decreased polyunsaturated fatty acids, attenuating its protective effect against LVTA, and in turn exacerbating VT or VF.[26] In addition, elevated fatty acid oxidation in LVTA may inhibit aerobic oxidation of glucose, thereby enhancing anaerobic glycolysis[27] and resulting in the increase of lactate observed here (Fig.4, Table 1). A high fatty acid oxidation rate combined with a low glucose oxidation rate would decrease cardiac efficiency

and impair heart function,[22, 27] which might be another factor contributing to heart collapse during LVTA.

Significant alteration of 10 amino acids (AAs) is another noticeable metabolic characteristic in myocardia of LVTA rats (Fig 4.). AAs serve a variety of biological functions. The change of AAs might reflect some key pathophysiological pathways of LVTA. First, all BCAAs are significantly decreased in myocardia post LVTA, which is consistent with cardiac ischemia involving BCAA catabolism.[28] BCAAs are catabolized only in non-hepatic organs, such as myocardium and muscle, and can serve as important bioenergetic fuel in energy-sensitive organs, such as heart and brain under stress conditions. When trembling, due to an exhaustion of fatty acid energy sources and stress, the heart has to utilize more BCAAs or other amino acids to supply energy on a priority basis,[29] resulting in higher catabolism, great consumption, and significantly lower level of all BCAAs. In addition, BCAA hemostasis is critical to maintain normal heart function and protect the heart under pathological conditions, mainly through defense against reactive oxygen species or inhibiting Ca^{2+} overload in the ischemic myocardium.[30] Decreased levels and imbalances of BCAAs would decrease their protective effect on the heart during LVTA, leading to ionic imbalance, forming a vicious cycle leading to fatal arrhythmia. Second, high glutamate is found in LVTA rats, which is confirmed to be able to activate the generation of NO synthesized from arginine by the NO synthase.[31] The latter is a sign of oxidative stress, and it has been suggested by high reactive oxygen species (ROS) in myocardia and malondialdehyde (MDA) in serum of LVTA rats (data no shown). In addition, excessive glutamate release is related to cell death post ischemia,[32] which may also be a metabolic mechanism leading to myocytes death during LVTA. Third, tyrosine and phenylalanine is decreased in myocardium of LVTA rats. As aromatic AAs, their main function is to synthesize catecholamine during sympathetic nerve excitation, and the latter can be confirmed by faster heart rate during LVTA.[33] Thus, lower level of tyrosine and phenylalanine might be a result of sympathetic nerve excitation during LVTA.

One more intriguing finding is that both fatty acids and BCAAs are located in the center of an interactive network established by cross correlation coefficient of all differential metabolites. Furthermore, all these metabolites are highly correlated with each other (Supplementary Fig. S5). BCAA catabolism and fatty acid oxidation mutually supply energy in skeletal muscle under exercising conditions.[30] The current results indicate that fibrillating myocardium, similar to exercising muscle, also derives energy from BCAA catabolism and fatty acid oxidation to enhance or maintain the capacity of the heart. A further explanation for their interaction is that enhanced catabolism of BCAAs leads to increased acetyl-CoA, enhanced TCA activity, and consequent inhibition of pyruvate dehydrogenase, shifting substrate oxidation toward increased lipid oxidation and away from the use of carbohydrates, which is partially supported by the current results. First, several TCA intermediates, such as succinate, fumarate, and malate are elevated in LVTA, which is possibly a consequence of increased acetyl-CoA, enhanced TCA activity, and high BCAA catabolism. Second, lactate increases dramatically (Fig.3, Table 1), which may be due to an inhibition of pyruvate dehydrogenase, causing pyruvate to be metabolized into lactate. Last, succinate, fumarate, malate, and lactate also correlate with fatty acids and BCAAs during LVTA. In the clinic, increasing glucose oxidation by inhibiting fatty acid oxidation has been used to improve cardiac efficiency and function in relatively non-fatal conditions, such as cardiac ischemia and diabetic cardiomyopathy.[34, 35] The current results also suggest such a measure of moderately inhibiting fatty acids oxidation to maintain the capacity of heart under LVTA, and further imply a new strategy of combined supplement of polyunsaturated fatty acids, and BCAAs to prevent LVTA related SCD, or to serve as an adjuvant treatment once ventricular arrhythmia occurs.

Taken together, major pathways concerning the common differential metabolites of these two LVTA models are energy excessive consumption and deficit, ionic imbalance, oxidative stress, cardiac cytotoxicity and membrane injury. Noticeably, the change degree of differential metabolites in aconitine-induced LVTA rats is greater than those

of CAL-induced LVTA rats, for the reason that most disturbed pathways of LVTA are related to cardiac ischemia; in CAL-induced LVTA rats, their controls also has cardiac ischemia pathological basis, which can partially offset the alterations of differential metabolites.

Diagnostic potentials of differential metabolites

The metabolic alterations observed in the myocardia of our two LVTA rat models could have been caused by LVTA itself or the stimuli. Thus, to minimize false results, we only considered changes that occurred in both models, as possible biomarkers for LVTA (Table 1). ROC analysis was performed to select optimal cut-off point score for each metabolite, which occurred in both models, as possible biomarkers for LVTA (Table 1). Sixteen metabolites with top ROC curve AUC values (>0.74) were chosen based on the ACO-LVTA data and its control. After MDR analysis for their categorization and interaction, five metabolites have been selected with the most different core (Fig. 5A). LVTA cases have been successfully classified into subgroups using L-valine, L-leucine, and stearic acid by CRT analysis. A classifier based on these potential biomarkers enables the classification with a total precision of 92.9%, and a combined ROC curve value of 0.986 (Fig. 5 B). Furthermore, the metabolites are highly correlated with the duration of VT, VF, VT+VF, and arrhythmia score, which remarkably declined both in two LVTA models (Table 1, 2). Based on our results, we hypothesize that a metabolite-based approach might aid in differentiating LVTA cases and identification the cause of death in those SCD cases without witness in forensic practices, and might also provide some clues for the treatment for clinical purpose.

Study limitations

This is a descriptive study of the metabolic feature of LVTA, the involved mechanisms are speculated. Therefore, detailed studies are required to explore definitive metabolic mechanisms of LVTA. Second, the study lacks serologic data, inhibiting its translation into clinical practice. Thus, serologic data are urgently needed in future research.

Third, higher sensitivity instruments are needed to enlarge the scope of detection to screen more specific differential metabolites.

Conclusions

The study identifies a common metabolic feature of LVTA in two rat models. The pathways regarding the common metabolome of LVTA are energy excessive consumption and deficit, ionic imbalance, oxidative stress, cardiac cytotoxicity and membrane injury. Valine, stearic acid and leucine in myocardial tissue collectively enable a high precision to distinguish LVTA from its controls, might serve as potential biomarkers of LVTA offer novel preventive and therapeutic targets for LVTA-related SCDs, and also can assist in identifying the cause of death of SCD in forensic practices.

The authors declare that they have no conflict of interest.

Compliance with Ethical Standards This study was approved by the Medical Animal Care & Welfare Committee at Shantou University Medical College under reference no. SUMC 2013-020. All procedures were carried out in accordance with the Helsinki Declaration.

Author contributions: DW, XXW, GHZhang wrote the manuscript. XXW, DW, JYW, and JYL performed the experiments. XXW, DW, GHZhang, GHZhu，and RBS analyzed the data. DW, XJY designed the study. DW takes responsibility for the work as a whole.

References

1. A. Barsheshet, A. Brenyo, A. J. Moss and I. Goldenberg, Genetics of sudden cardiac death, *Current cardiology reports*, 2011, **13**, 364-376.
2. W. Hua, L. F. Zhang, Y. F. Wu, X. Q. Liu, D. S. Guo, H. L. Zhou, Z. P. Gou, L. C. Zhao, H. X. Niu, K. P. Chen, J. Z. Mai, L. N. Chu and S. Zhang, Incidence of sudden cardiac death in China: analysis of 4 regional populations,

Journal of the American College of Cardiology, 2009, **54**, 1110-1118.

3. N. Chopra and B. C. Knollmann, Genetics of sudden cardiac death syndromes, *Current opinion in cardiology*, 2011, **26**, 196-203.
4. M. Papadakis, S. Sharma, S. Cox, M. N. Sheppard, V. F. Panoulas and E. R. Behr, The magnitude of sudden cardiac death in the young: a death certificate-based review in England and Wales, *Europace : European pacing, arrhythmias, and cardiac electrophysiology : journal of the working groups on cardiac pacing, arrhythmias, and cardiac cellular electrophysiology of the European Society of Cardiology*, 2009, **11**, 1353-1358.
5. R. F. Marsman, H. L. Tan and C. R. Bezzina, Genetics of sudden cardiac death caused by ventricular arrhythmias, *Nat Rev Cardiol*, 2014, **11**, 96-111.
6. J. K. Nicholson, J. C. Lindon and E. Holmes, 'Metabonomics': understanding the metabolic responses of living systems to pathophysiological stimuli via multivariate statistical analysis of biological NMR spectroscopic data, *Xenobiotica; the fate of foreign compounds in biological systems*, 1999, **29**, 1181-1189.
7. J. L. Griffin, H. Atherton, J. Shockcor and L. Atzori, Metabolomics as a tool for cardiac research, *Nature reviews. Cardiology*, 2011, **8**, 630-643.
8. H. J. Heuer and W. Bernauer, Myocardial damage by ventricular fibrillation in isolated perfused rat hearts, and its underlying mechanisms, *Basic research in cardiology*, 1986, **81**, 188-198.
9. S. Neubauer, J. B. Newell and J. S. Ingwall, Metabolic consequences and predictability of ventricular fibrillation in hypoxia. A 31P- and 23Na-nuclear magnetic resonance study of the isolated rat heart., *Circulation*, 1992, **86**, 302-310.
10. J. A. Barrabes, D. Garcia-Dorado, F. Padilla, L. Agullo, L. Trobo, J. Carballo and J. Soler-Soler, Ventricular fibrillation during acute coronary occlusion is related to the dilation of the ischemic region, *Basic research in cardiology*, 2002, **97**, 445-451.
11. Y. Gao, J. Gao, C. Chen, H. Wang, J. Guo and R. Wu, Cardioprotective effect of polydatin on ventricular remodeling after myocardial infarction in coronary artery ligation rats, *Planta medica*, 2015, **81**, 568-577.
12. M. J. Curtis and M. J. Walker, Quantification of arrhythmias using scoring systems: an examination of seven scores in an in vivo model of regional myocardial ischaemia, *Cardiovascular research*, 1988, **22**, 656-665.
13. J. A, J. Trygg, J. Gullberg, A. I. Johansson, P. Jonsson, H. Antti, S. L. Marklund and T. Moritz, Extraction and GC/MS analysis of the human blood plasma metabolome, *Analytical chemistry*, 2005, **77**, 8086-8094.
14. E. C. Chan, P. K. Koh, M. Mal, P. Y. Cheah, K. W. Eu, A. Backshall, R. Cavill, J. K. Nicholson and H. C. Keun, Metabolic profiling of human colorectal cancer using high-resolution magic angle spinning nuclear magnetic resonance (HR-MAS NMR) spectroscopy and gas chromatography mass spectrometry (GC/MS), *Journal of proteome research*, 2009, **8**, 352-361.
15. C. L. Gavaghan, E. Holmes, E. Lenz, I. D. Wilson and J. K. Nicholson, An NMR-based metabonomic approach to investigate the biochemical consequences of genetic strain differences: application to the C57BL10J and Alpk:ApfCD mouse, *FEBS letters*, 2000, **484**, 169-174.
16. S. Serres, E. Bezancon, J. M. Franconi and M. Merle, Ex vivo analysis of lactate and glucose metabolism in the rat brain under different states of depressed activity, *The Journal of biological chemistry*, 2004, **279**, 47881-47889.
17. S. H. Kim, S. O. Yang, H. S. Kim, Y. Kim, T. Park and H. K. Choi, 1H-nuclear magnetic resonance spectroscopy-based metabolic assessment in a rat model of obesity induced by a high-fat diet, *Anal*

Bioanal Chem, 2009, **395**, 1117-1124.

18. M. D. Ritchie, L. W. Hahn, N. Roodi, L. R. Bailey, W. D. Dupont, F. F. Parl and J. H. Moore, Multifactor-dimensionality reduction reveals high-order interactions among estrogen-metabolism genes in sporadic breast cancer, *American journal of human genetics*, 2001, **69**, 138-147.
19. S. Y. Jung, M. Z. Vitolins, J. Fenton, A. C. Frazier-Wood, S. D. Hursting and S. Chang, Risk profiles for weight gain among postmenopausal women: a classification and regression tree analysis approach, *PloS one*, 2015, **10**, e0121430.
20. C. M. Albert, C. U. Chae, F. Grodstein, L. M. Rose, K. M. Rexrode, J. N. Ruskin, M. J. Stampfer and J. E. Manson, Prospective study of sudden cardiac death among women in the United States, *Circulation*, 2003, **107**, 2096-2101.
21. T. Rankinen, M. A. Sarzynski, S. Ghosh and C. Bouchard, Are there genetic paths common to obesity, cardiovascular disease outcomes, and cardiovascular risk factors?, *Circ Res*, 2015, **116**, 909-922.
22. D. Abdurrachim, J. J. Luiken, K. Nicolay, J. F. Glatz, J. J. Prompers and M. Nabben, Good and bad consequences of altered fatty acid metabolism in heart failure: evidence from mouse models, *Cardiovascular research*, 2015, **106**, 194-205.
23. M. Calvani, E. Reda and E. Arrigoni-Martelli, Regulation by carnitine of myocardial fatty acid and carbohydrate metabolism under normal and pathological conditions, *Basic Res Cardiol*, 2000, **95**, 75-83.
24. V. Bodi, V. G. Marrachelli, O. Husser, F. J. Chorro, J. R. Viña and D. Monleon, Metabolomics in the diagnosis of acute myocardial ischemia, *J Cardiovasc Transl Res*, 2013, **6**, 808-815.
25. M. F. Murnaghan, Effect of fatty acids on the ventricular arrhythmia threshold in the isolated heart of the rabbit, *Br J Pharmacol*, 1981, **73**, 909-915.
26. Y. F. Xiao, D. C. Sigg and A. Leaf, The antiarrhythmic effect of n-3 polyunsaturated fatty acids: modulation of cardiac ion channels as a potential mechanism, *J Membr Biol*, 2005, **206**, 141-154.
27. N. Fillmore, J. Mori and G. D. Lopaschuk, Mitochondrial fatty acid oxidation alterations in heart failure, ischaemic heart disease and diabetic cardiomyopathy, *British journal of pharmacology*, 2014, **171**, 2080-2090.
28. K. J. Drake, V. Y. Sidorov, O. P. McGuinness, D. H. Wasserman and J. P. Wikswo, Amino acids as metabolic substrates during cardiac ischemia, *Exp Biol Med (Maywood)*, 2012, **237**, 1369-1378.
29. Y. Huang, M. Zhou, H. Sun and Y. Wang, Branched-chain amino acid metabolism in heart disease: an epiphenomenon or a real culprit?, *Cardiovascular research*, 2011, **90**, 220-223.
30. G. D'Antona, M. Ragni, A. Cardile, L. Tedesco, M. Dossena, F. Bruttini, F. Caliaro, G. Corsetti, R. Bottinelli, M. O. Carruba, A. Valerio and E. Nisoli, Branched-chain amino acid supplementation promotes survival and supports cardiac and skeletal muscle mitochondrial biogenesis in middle-aged mice, *Cell Metab*, 2010, **12**, 362-372.
31. M. Castellanos, T. Sobrino, S. Pedraza, O. Moldes, J. M. Pumar, Y. Silva, J. Serena, M. Garcia-Gil, J. Castillo and A. Davalos, High plasma glutamate concentrations are associated with infarct growth in acute ischemic stroke, *Neurology*, 2008, **71**, 1862-1868.
32. N. Chao and S. T. Li, Synaptic and extrasynaptic glutamate signaling in ischemic stroke, *Current medicinal chemistry*, 2014, **21**, 2043-2064.
33. E. Akil, Y. Tamam, M. A. Akil, I. Kaplan, M. Z. Bilik, A. Acar and B. Tamam, Identifying autonomic nervous system dysfunction in acute cerebrovascular attack by assessments of heart rate variability and

catecholamine levels, *Journal of neurosciences in rural practice*, 2015, **6**, 145-150.
34. G. D. Lopaschuk, J. R. Ussher, C. D. Folmes, J. S. Jaswal and W. C. Stanley, Myocardial fatty acid metabolism in health and disease, *Physiol Rev*, 2010, **90**, 207-258.
35. W. C. Stanley and H. N. Sabbah, Metabolic therapy for ischemic heart disease: the rationale for inhibition of fatty acid oxidation, *Heart failure reviews*, 2005, **10**, 275-279.

Figure Legends

Figure. 1 *Lead II ECG in each LVTA rat model.* ***A2 A3*** *VT and VF occur in 2-5 minutes after aconitine injection through the tail vein.* ***B2 B3*** *VT and VF occur in 4-6 minutes after CAL.* ***C3*** *Severe bradycardia after CAL-myocardial ischemia.* ***D2*** *Severe bradycardia induced by pentobarbital sodium over-anesthetization.* ***A1-D1*** *Normal ECGs before treatment.*

Figure. ***2*** *PLS-DA models. Two-component plot of LVTA induced by aconitine and its control (green circle=aconitine, blue square=control) from GC-MS (**A**) and 1H-NMR (**B**) metabolic profiles; both demonstrate clear separation from each other. Three-component plot in three CAL groups (green=CAL-T, pink=CAL-M, blue=CAL-N) from GC-MS (**C**) and 1H-NMR (**D**) metabolic profiles show clear distinction among these groups. The results indicate a significant difference in myocardia metabolic profiles between the aconitine-LVTA group and its control, and among the three CAL groups.*

Figure. 3 *Heat map of the 38 potential differential metabolites between ACO-LVTA and its control (PI), and between CAL-T and CAL-N. The colors from green to red in each square indicate a ratio of differential metabolite content in each LVTA myocardial sample to the average content of corresponding metabolite in control. Here, the data of GC-MS and 1H NMR had been integrated, so the sample numbers of ACO-LVTA rats and CAL-T rats are sixteen and thirteen, respectively).*

Figure. 4 *Metabolic network of significantly changed metabolites between ACO-LVTA and its control The normalized contents are shown under the chemical name. Red and green represent significantly elevated and reduced metabolites in ACO-LVTA compared with its control. All P values were calculated by Student's test. *, P<0.05; **, P<0.01; ***, P<0.001. Unchanged metabolites are shown in black. The names with a dashed line frame represent undetected metabolites. ACO, aconitine-LVTA group; PI, control group over-anesthetized with pentobarbital injection; GPC, glycerophosphocholine.*

Figure. 5 Diagnostic potential for LVTA of differential metabolites. *A MDR analysis of 16 differential metabolites having an AUC of more than 0.74, metabolites with blue color, consist of leucine, phosphate, glutamate, sulfite, and valine, mean they have core value to discriminate the LVTA from the control. B ROC curves, of L-valine, L-leucine, stearic acid and the combination of three metabolites, for distinguishing LVTA-SCD from the pentobarbital over-anesthetized death control. C CRT analysis from lactate, succinate, L-valine, leucine, and stearic acid.*

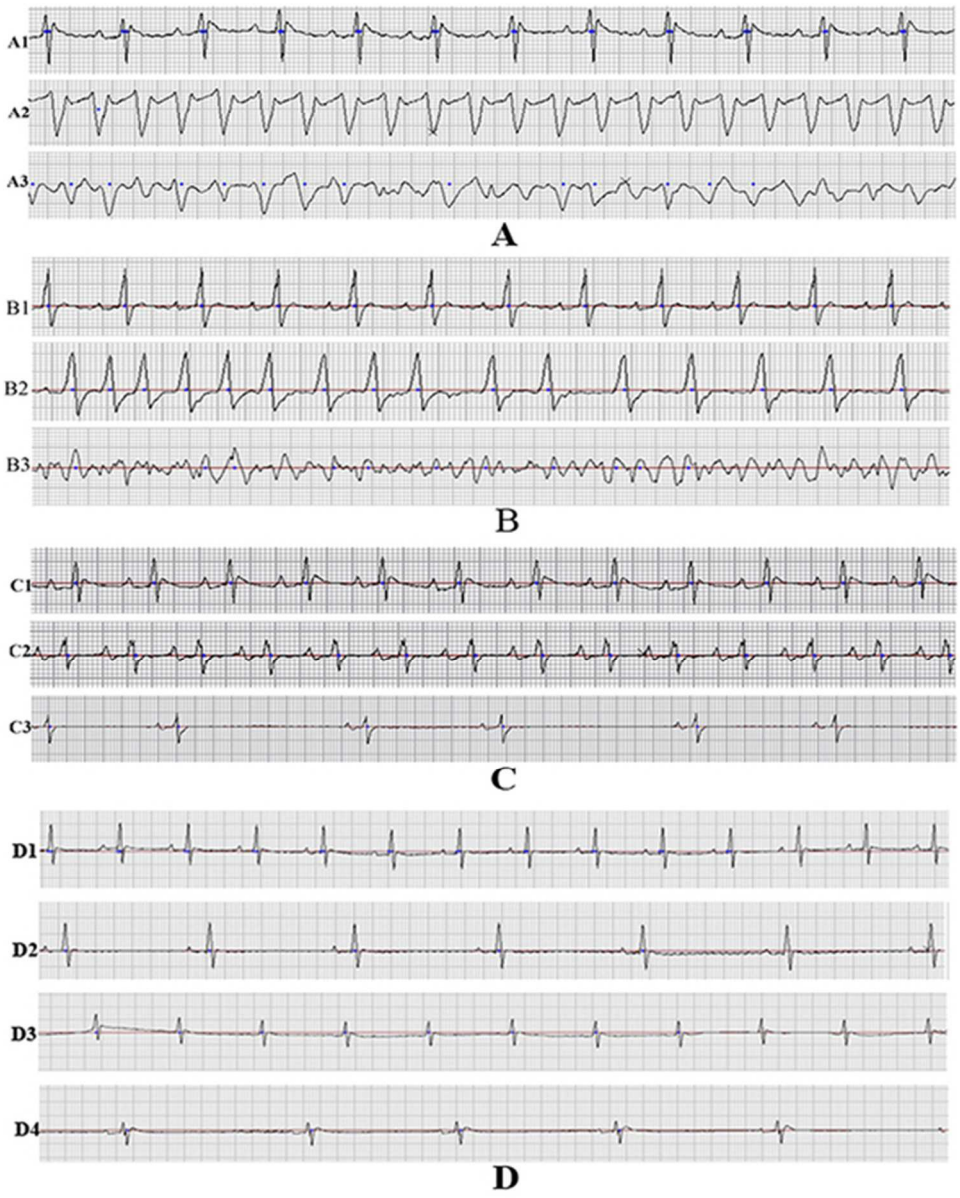

49x62mm (300 x 300 DPI)

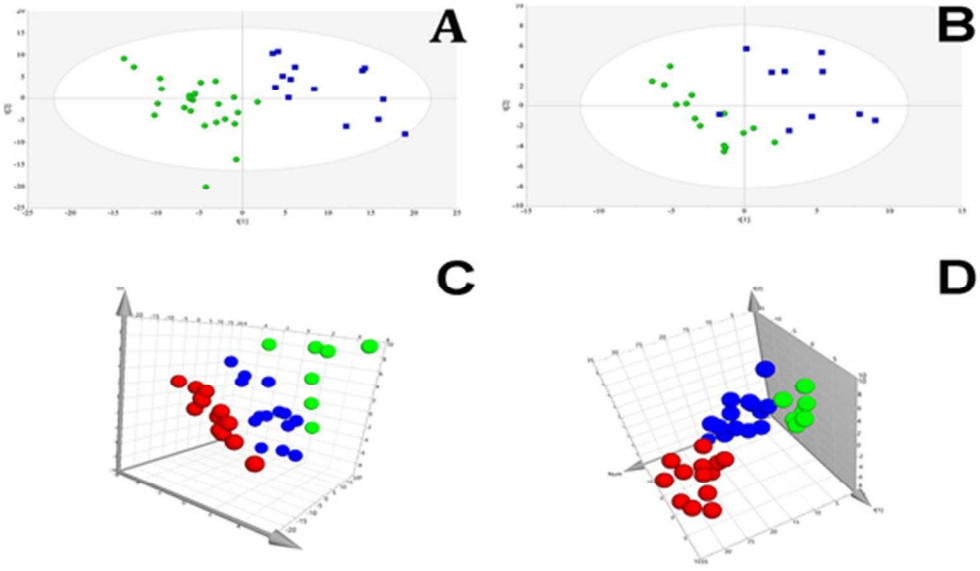

49x29mm (300 x 300 DPI)

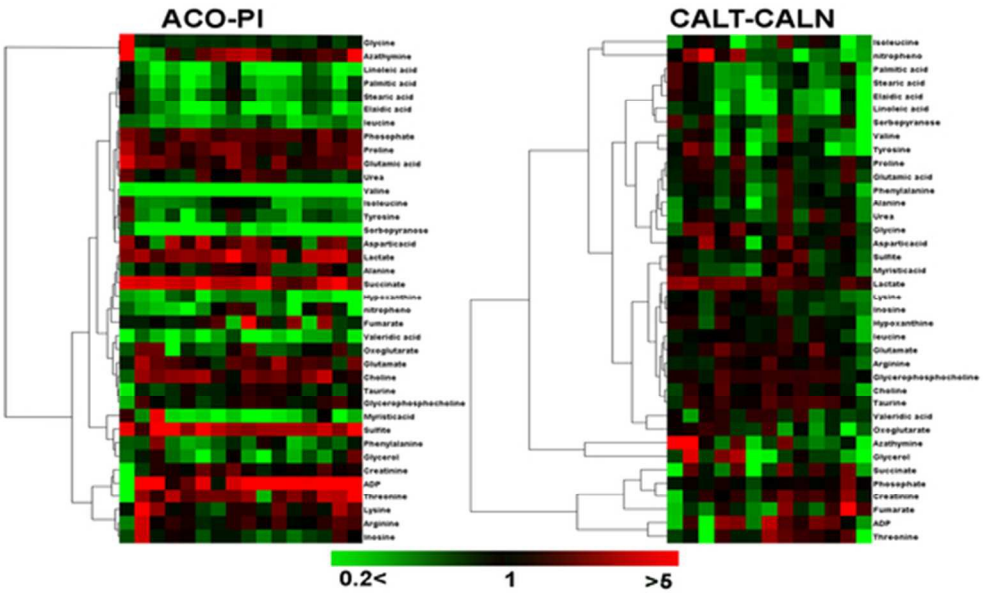

49x29mm (300 x 300 DPI)

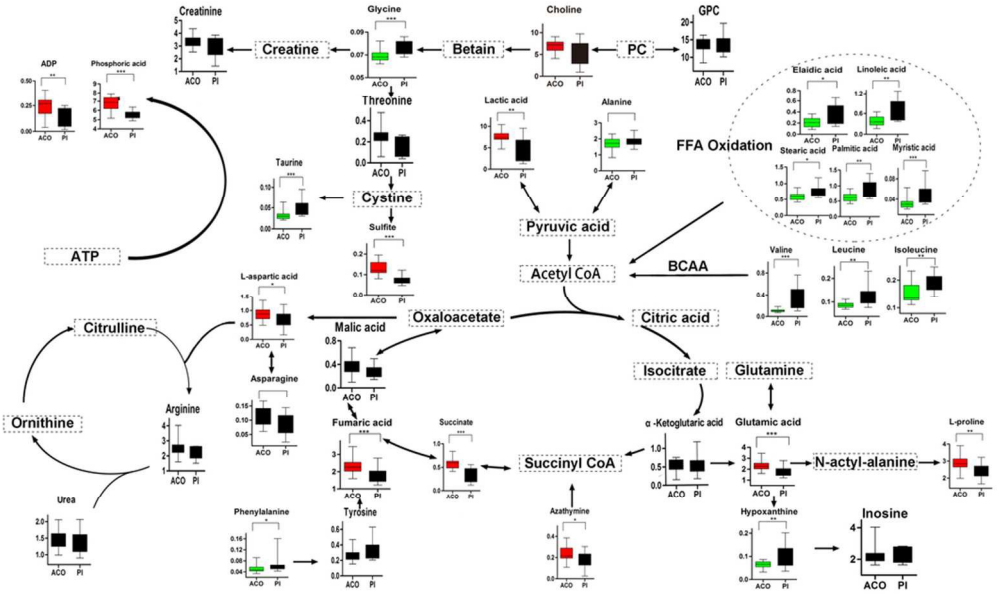

90x54mm (300 x 300 DPI)

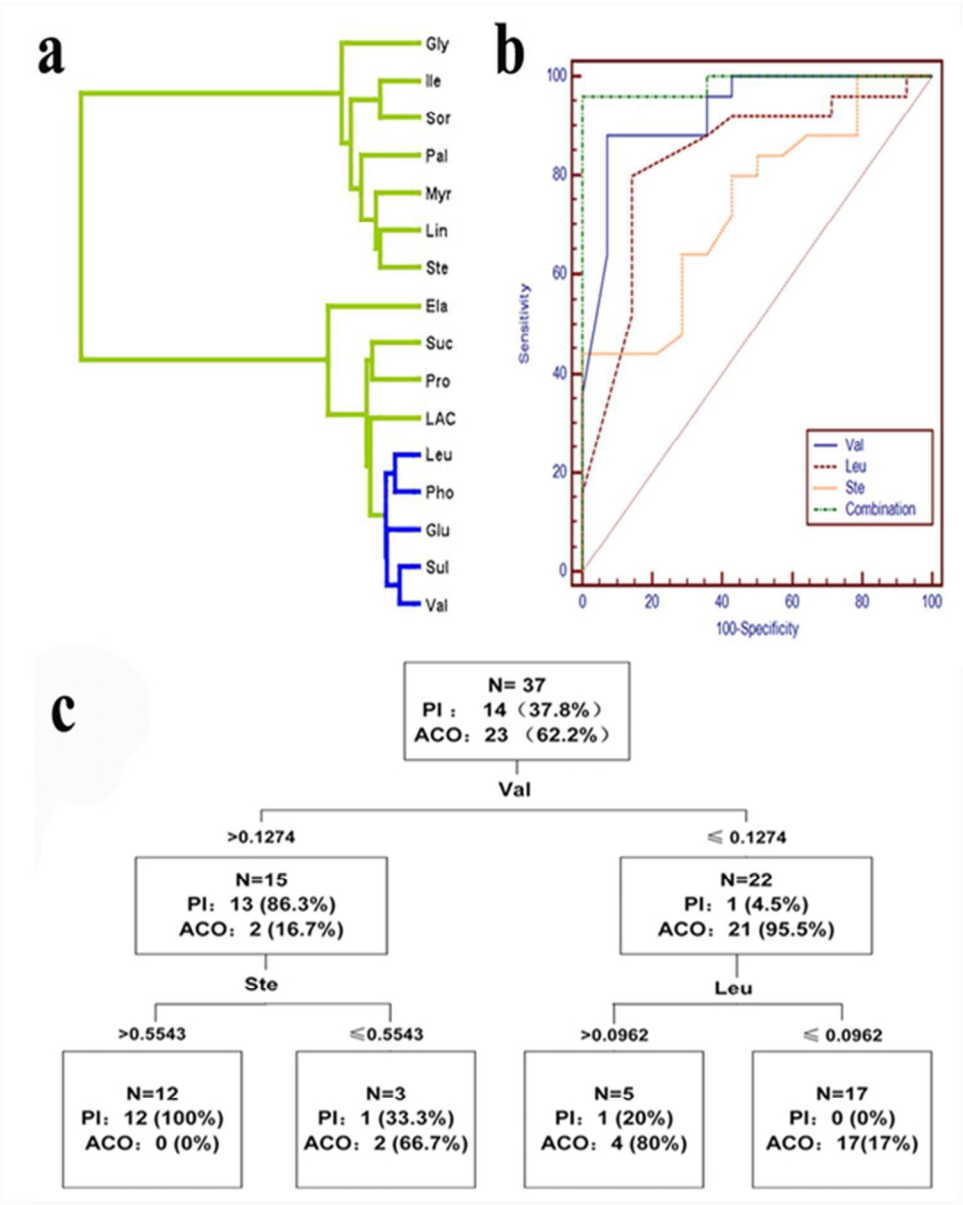

49x62mm (300 x 300 DPI)

Table 1. Comparison of significantly different metabolites between two models by two tests

Model I								*Model II*							
Discovery test (GC-MS)				*Validation test (1H-NMR)*				*Discovery test (GC-MS)*				*Validation test (1H-NMR)*			
Metabolites	***P***	***FC***	***VIP***	***Metabolites***	***P***	***FC***	***VIP***	***Metabolites***	***P***	***FC***	***VIP***	***Metabolites***	***P***	***FC***	***VIP***
lactic acid	0.04	1.33	1.23	Lactic acid	0.03	1.38	4.09	Lactic acid	0.02	1.31	1.77	Lactic acid	0.58	1.16	
L-valine	0.00	0.35	1.54	L-valine	0.04	0.55	2.98	L-valine	0.10	0.81		L-valine	0.37	0.95	
Isoleucine	0.00	0.78		Isoleucine	0.00	0.24	1.41	Isoleucine	0.20	0.78		Isoleucine	0.53	0.98	
L-leucine	0.00	0.67		L-leucine	0.01	0.59	1.28	L-leucine	0.82	0.95		L-leucine	0.08	0.85	0.95
Phosophate	0.00	1.23	1.80	ADP	0.80	1.99	1.69	Phosophate	0.30	1.05	1.05	ADP	0.02	1.10	
L-proline	0.01	1.18	1.04	Choline	0.01	1.30		L-proline	0.55	1.04		Choline	0.56	1.02	2.53
Glutamate	0.00	1.29	1.20	Valeric acid	<0.001	0.58		Glutamate	0.88	1.00	0.77	Valeric acid	0.09	0.95	
Palmitic acid	0.00	0.71	1.35	Glycerol	0.30	0.80	1.17	Palmitic acid	0.09	0.81	1.04	Glycerol	0.00	0.69	3.11
Linoleic acid	0.00	0.58	1.42	Glucose	0.88	0.86		Linoleic acid	0.06	0.63		Glucose	0.00	0.85	
Elaidic acid	0.04	0.61	1.33	Lysine	0.23	1.22	0.89	Elaidic acid	0.37	0.68		Lysine	0.05	0.92	
Stearic acid	0.01	0.80	1.31	Glutamate	0.07	1.19	1.07	Stearic acid	0.04	0.75	1.45	Glutamate	0.46	1.10	0.83
Succinate	000	1.53	1.24	Succinate	0.24	1.38	0.87	Succinate	0.82	0.96		Succinate	0.83	0.90	1.00
Sorbopyranose	0.01	0.45		Taurine	0.12	0.94	2.42	Sorbopyranose	0.30	0.91		Taurine	0.23	1.12	1.23
Sulfite	0.00	1.84		Arginine	0.90	1.11	0.78	Sulfite	0.55	0.96		Arginine	0.73	1.00	2.34
Glycine	0.00	1.15		Inosine	0.64	0.96	1.15	Glycine	0.65	0.99		Inosine	0.08	0.91	
Azathymine	0.03	1.65		Oxoglutarate	0.59	1.14		Azathymine	0.88	1.28		Oxoglutarate	0.59	0.88	1.13
Phenylalanine	0.02	0.79		Creatine	0.95	0.83	0.94	Phenylalanine	0.16	0.89		Creatine	0.90	1.03	
Myristic acid	0.00	0.68		Threonine	0.37	1.37	0.84	Myristic acid	0.30	0.91		Threonine	0.36	1.00	0.80
Creatinine	0.32	1.10	1.27	Ethanol	0.01	0.85		Creatinine	0.50	0.79		Ethanol	0.64	1.14	
Aspartic acid	0.04	1.31		Glycerophosphocholine	0.20	1.01	0.80	Aaspartic acid	0.60	1.06		Glycerophosphocholine	0.21	1.12	1.63
L-alanine	0.77	0.90	1.18	Hypoxanthine	0.01	0.62		L-alanine	0.12	0.86		Hypoxanthine	0.95	0.98	
Urine	0.41	1.05	1.08					Urine	0.60	0.96					
Tyrosine	0.17	0.82	0.93					Tyrosine	0.33	1.48					
Fumarate	0.86	1.53						Fumarate	0.60	0.81	0.96				
Cholesterol	0.80	0.79	0.80					Cholesterol	0.31	1.30					

Metabolites displaying significant changes in levels ($P<0.05$ and/or VIP $\geqq 0.75$) were selected and compared between two models by two tests. P, Student's test between the LVTA group and its control in both models. FC, fold change; VIP, variable Importance in the projection.

Table 2 Correlation of the top 16 AUC metabolites and their arrhythmia indices, and related pathways and enzymes

Metabolites	AUC	R^2 (VT)	R^2 (VF)	R^2 (VT/VF)	R^2 (AS)	Pathways	Enzymes
Phosphoric acid	0.929	0.30*	0.40**	0.37**	0.38**	Oxidative phosphorylation	
L-valine	0.927	-0.43**	-0.41**	-0.47**	-0.54**	Valine, leucine and isoleucine degradation	Valine dehydrogenase
Sulfite	0.919	0.27*	0.44**	0.36**	0.35**	Cysteine and methionine metabolism	sulfite reductase
L-leucine	0.833	-0.26*	-0.44**	-0.39**	-0.40**	Valine, leucine and isoleucine degradation	Leucine dehydrogenase
Myristic acid	0.823	0.02	-0.18	-0.06	0.02	Fatty acid degradation	long-chain acyl-CoA synthetase
Glutamatic acid	0.823	0.03	0.31**	0.19	0.13	Alanine, aspartate and glutamate metabolism	glutamate dehydrogenase
Succinic acid	0.819	0.07	0.19	0.15	0.12	Tricarboxylic acid cycle	Succinate-semialdehyde dehydrogenase
Lactic acid	0.806	0.14	0.29*	0.22	0.14	Glycolysis and gluconeogenesis	Lactate dehydrogenase
Isoleucine	0.787	-0.35**	-0.22	-0.35**	-0.45**	Valine, leucine and isoleucine degradation	L-amino-acid oxidase
Linoleic acid	0.786	-0.18	-0.24*	-0.25*	-0.35**	Linoleic acid metabolism	lipoxygenase
Palmitic acid	0.780	-0.24*	-0.34**	-0.32**	-0.39**	Fatty acid degradation	long-chain acyl-CoA synthetase
Glycine	0.777	-0.34**	-0.13	-0.27*	-0.37**	Glycine, serine and threonine metabolism	Threonine aldolase
Proline	0.774	0.10	0.28*	0.21	0.16	Arginine and proline metabolism	Proline oxidase
Sorbinose	0.771	-0.28*	-0.16	-0.25*	-0.34**		
Elaidic acid	0.763	-0.18	-0.24*	-0.25*	-0.35**	Fatty acid degradation	long-chain acyl-CoA synthetase
Stearic acid	0.740	-0.25*	-0.37**	-0.37**	-0.44**	Fatty acid degradation	long-chain acyl-CoA synthetase

AUC stands for area under curve (AUC) of ROC to distinguish ACO-LVTA from its control. R^2 is the Spearman correlation coefficient between the relative amount of the metabolites and arrhythmia index, including the duration (seconds) of VT, VF, and VT+VF, and arrhythmia score in the experimental rats. * and ** mean correlations are significant at a 0.05 and 0.01 level, respectively.